



GEOMETRICALLY NON-LINEAR TRANSIENT ANALYSIS OF LAMINATED COMPOSITE AND SANDWICH SHELLS WITH A REFINED THEORY AND C^0 FINITE ELEMENTS

T. Kant† and J. R. Kommineni

Department of Civil Engineering, Indian Institute of Technology, Powai, Bombay-400076, India

(Received 29 January 1993)

Abstract—A C^0 continuous finite element formulation of a higher order shear deformation theory is presented for predicting the linear and geometrically non-linear, in the sense of von Karman, transient responses of composite and sandwich laminated shells. The displacement model accounts for the non-linear cubic variation of the tangential displacement components through the thickness of the shell and the theory requires no shear correction coefficients. In the time domain, the explicit central difference integrator is used in conjunction with the special mass matrix diagonalization scheme which conserves the total mass of the element and includes effects due to rotary inertia terms. Numerical results for central transverse deflection and stresses are presented for composite and sandwich laminated shells with various boundary conditions subjected to different types of loads and are compared with the results from other sources. Some new results are also included for future reference.

INTRODUCTION

At present, due to the increased use of composite materials in the aerospace and automotive industries because of their superior mechanical properties such as high stiffness per unit weight, high strength per unit weight and potentially low unit cost, a need has arisen for a basic understanding of their response to dynamic loading. Because of the high modulus and high strength properties that composites have, structural composites undergo large deformations before they become inelastic. Therefore, an accurate prediction of transient response is possible only when one accounts for the geometric non-linearity. Hence, studies involving the assessment of the geometrically non-linear transient response of composite and sandwich laminated shells are receiving much attention by composite structural engineers.

Classical lamination theories are based on the Love-Kirchhoff hypothesis, in which transverse shear deformation effects are neglected, and surveys of such theories can be seen in the works of Naghdi [1]. The neglect of transverse shear strains in composite laminates could lead to an underestimation of the deflections and stresses and an overestimation of the natural frequencies and critical buckling loads because of the low transverse shear moduli. In a non-linear context Horrigmoe and Bergan [2] presented classical variational principles for non-linear problems by considering the incremental deformations of a continuum.

To counter the above drawbacks in classical lamination theories, a first order shear deformation theory is used in which constant shear strains through the thickness are established. Since the actual shear strain variation is non-linear over the thickness of a shell, shear correction coefficients are used in the energy expression. Such theories when applied to layered anisotropic shells for bending, stability and vibration problems can be found in the works of Panda and Natarajan [3], Shivakumar and Krishna Murty [4], Rao [5], Hsu *et al.* [6], Reddy [7]. Reddy and Chandrashekhara [8, 9] presented a geometric non-linear transient response of composite doubly curved shells with such a first order shear deformation theory.

For sandwich laminates of weak core and comparatively strong facings and highly anisotropic laminates, the shear deformation effect is much more pronounced. Refined theories were established to account for these effects. Hildebrand *et al.* [10] were the first to make significant contributions by dispensing with all Love's assumptions and assuming a three term Taylor's series expansion for the displacement vector. By including the second order shear deformation effects Kant [11] developed a complete governing set of equations of a general thick shell theory. The theory is based on Hildebrand *et al.* [10] and is applicable to orthotropic material laminae having planes of symmetry coincident with the shell coordinates. Whitney and Sun [12] developed a refined shell theory in which the displacements in the surface of the shell are expanded as linear functions of the thickness coordinate and the transverse displacement

† Author to whom correspondence should be addressed.

is expanded as a quadratic function of the thickness coordinate. Kant [13, 14] presented higher order theories for general orthotropic as well as laminated shells, which are derived by expanding the displacement vector by the powers of the thickness coordinate. These theories account for the effects of the transverse shear deformation, transverse normal stress and transverse normal strain with the implicit non-linear distribution of the tangential displacement components through the thickness of the shell. Kant *et al.* [15] presented a C^0 finite element formulation of a higher order theory. Reddy *et al.* [16–18] presented a third order shear deformation theory in which the surface displacements are expanded up to the cubic term in the thickness coordinate, while the transverse deflection is assumed to be constant through the thickness. The nine undetermined functions are reduced to seven by imposing shear stress free boundary conditions on the bounding surfaces of the shell. With this the displacement based finite element model adopted by Reddy gives rise to second order derivatives of the transverse displacement in the energy expression and hence a displacement based finite element formulation requires C^1 continuous shape functions which are difficult to derive, computationally inefficient and not amenable to the popular and widely used isoparametric formulation in the present day finite element technology. Recently Kant and Kommineni [19] presented a displacement based higher order shear deformation theory for the linear and geometrically non-linear static analysis of laminated composite and sandwich shells by using C^0 finite elements. Kant and Mallikarjuna [20] presented the dynamic large deflection response of laminated composite plates using higher order shear deformation theory with seven degrees of freedom per node.

Kant [20–30] along with co-workers emphasized the C^0 finite element formulation of the refined higher order shear deformation theories for the static and dynamic linear analysis of layered generally orthotropic plates and shells. They have established the credibility of such a formulation after doing extensive numerical investigations on composite and sandwich laminates. They have confirmed that the imposition of shear free boundary conditions at the top and bottom bounding planes of the laminate gives stiffer solutions when compared to exact solutions especially in the case of thick laminates [29, 30]. Further they have also concluded that among the various displacement models for flat laminates, the one having nine degrees of freedom per node produces results very close to the exact solutions [20–30]. As regards curved laminates, work is in progress and a definite conclusion should emerge after some more investigation.

To the authors' knowledge there is no evidence of any published work on the use of a higher order shear deformation theory with C^0 finite elements for predicting the linear and geometrically non-linear transi-

ent responses of composite and sandwich laminated shells. In this paper a third order shear deformation theory is constructed in which the tangential displacement components are cubic functions of the thickness z coordinate whereas the transverse displacement component is assumed to be constant through the thickness of the shell. The effect of geometric non-linearity is included in the formulation by adopting the von Karman assumptions. In addition to the higher order shear deformation theory, a first order shear deformation theory by incorporating first order shear deformation effects in Sander's thin shell theory is developed to enable a comparison of the results of the present formulation with a parallel formulation and also to study the shear deformation effects especially in sandwich shells. Several examples drawn from the literature are analysed and appropriate comparisons are made to show the simplicity, validity and accuracy of the present formulation.

THEORY AND FORMULATION

A fibre reinforced composite shell consisting of isotropic/orthotropic laminae oriented arbitrarily having a total thickness of h with $h_1, h_2, h_3, \dots, h_n$, etc., being the thicknesses of individual layers such that $h = h_1 + h_2 + h_3 + \dots + h_n$ is considered. Symbols x, y are the curvilinear dimensional coordinates defining the mid-surface of the shell and the z -axis is oriented in the thickness direction as shown in Fig. 1.

In the present theory displacement components of a generic point in the composite shell are assumed to be of the form

$$\begin{aligned} u(x, y, z, t) &= u_0(x, y, t) + z\theta_x(x, y, t) \\ &\quad + z^2u_0^*(x, y, t) + z^3\theta_x^*(x, y, t) \\ v(x, y, z, t) &= v_0(x, y, t) + z\theta_y(x, y, t) \\ &\quad + z^2v_0^*(x, y, t) + z^3\theta_y^*(x, y, t) \\ w(x, y, z, t) &= w_0(x, y, t), \end{aligned} \quad (1)$$

where u_0, v_0 and w_0 are the middle surface displacements of a generic point having displacements u, v and w in the x, y and z directions respectively. The parameters θ_x and θ_y are the rotations of the transverse normal in the xz and yz surfaces respectively. The parameters u_0^*, v_0^*, θ_x^* and θ_y^* are the higher order terms in the Taylor's series expansion and they represent the higher order transverse cross-sectional deformation modes. The mid-surface displacement components $u_0, v_0, w_0, \theta_x, \theta_y, u_0^*, v_0^*, \theta_x^*$ and θ_y^* are the nine degrees of freedom of the present higher order displacement model.

A total Lagrangian approach is adopted and the stress and strain descriptions used are those due to Piola–Kirchhoff and Green respectively. The present theory includes large displacements in the sense of

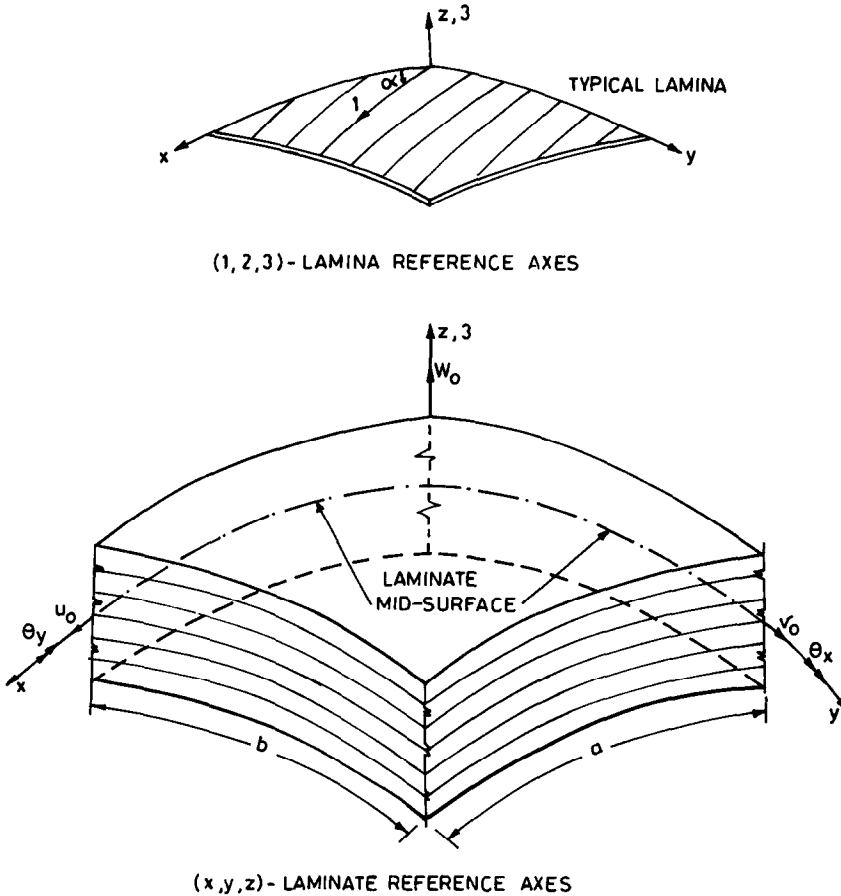


Fig. 1. Laminate geometry with positive set of lamina/lamina reference axes, displacement components and fibre orientation.

von Karman, which in particular imply that the first order derivatives of the tangential displacement components with respect to the x, y and z are small so that their particular products can be neglected (see Reddy and Chandrashekhara [8, 9]). The following are the strain displacement relations (see Novozhilov [31])

$$\begin{aligned}
 \epsilon_x &= \frac{\partial u}{\partial x} + \frac{w}{R_1} + \frac{1}{2} \left(\frac{\partial w}{\partial x} \right)^2 \\
 \epsilon_y &= \frac{\partial v}{\partial y} + \frac{w}{R_2} + \frac{1}{2} \left(\frac{\partial w}{\partial y} \right)^2 \\
 \gamma_{xy} &= \frac{\partial u}{\partial y} + \frac{\partial v}{\partial x} + \frac{\partial w}{\partial x} \frac{\partial w}{\partial y} \\
 \gamma_{xz} &= \frac{\partial u}{\partial z} + \frac{\partial w}{\partial x} - \frac{u}{R_1} \\
 \gamma_{yz} &= \frac{\partial v}{\partial z} + \frac{\partial w}{\partial y} - \frac{v}{R_2}
 \end{aligned}
 \tag{2}$$

To develop the equations of motion of a composite and sandwich laminated shell, Hamilton's variational principle is used here. According to Hamilton's vari-

ational principle, the first variation of the Lagrangian function, L_f must vanish, i.e.

$$\delta \int_{t_1}^{t_2} L_f dt = 0, \tag{3}$$

in which $L_f = \Pi - E$, where δ is the variation taken during the indicated time interval and the integral of L_f takes an extreme value which can be shown to be a minimum. The parameters E and Π define the kinetic and potential energies of the system, respectively.

The potential energy Π of the system can be written as

$$\begin{aligned}
 \Pi &= U - W \\
 &= \frac{1}{2} \int_V \epsilon' \sigma dv - \int_V \mathbf{u}' \mathbf{F} dv - \int_S \mathbf{u}' \mathbf{T}^* ds, \tag{4a}
 \end{aligned}$$

where U is internal strain energy, W is the work done by the applied loads during the deformation, and the vector \mathbf{u} represents three displacement components u, v and w of a point, the external forces \mathbf{F} and \mathbf{T}^* are body force components and surface traction respectively and S is the portion of the body on which the tractions are prescribed.

The kinetic energy of the body E can be written as

$$E = \frac{1}{2} \int_V \dot{\mathbf{u}}' \rho \dot{\mathbf{u}} \, dv, \tag{4b}$$

where ρ is the mass density of the material and $\dot{\mathbf{u}}$ defines the particle velocity vector. Equation (3) is then rewritten as

$$\delta \int_{t_1}^{t_2} \left(\frac{1}{2} \int_V \epsilon' \sigma \, dv - \int_V \mathbf{u}' \mathbf{F} \, dv - \int_S \mathbf{u}' T^* \, ds - \frac{1}{2} \int_V \dot{\mathbf{u}}' \rho \dot{\mathbf{u}} \, dv \right) dt = 0. \tag{5a}$$

Thus, the mathematical statement of Hamilton's variational principle can be written as

$$\int_{t_1}^{t_2} (\delta U - \delta W - \delta E) \, dt = 0, \tag{5b}$$

where δU , δE and δW are the first variations of the strain energy, kinetic energy and the work done by the external loads respectively.

The constitutive equations of the L th lamina in the lamina reference axes (1, 2, 3) can be written as follows:

$$\begin{aligned} C_{22} &= \left(\frac{E_2}{1 - \nu_{12} \nu_{21}} \right); \\ C_{33} &= G_{12}; \quad C_{44} = G_{13}; \\ C_{55} &= G_{23} \quad \text{with} \quad \frac{\nu_{12}}{E_1} = \frac{\nu_{21}}{E_2}. \end{aligned} \tag{6c}$$

If the principal material axes (1, 2) of a lamina do not coincide with the reference axes of the laminated shell (x, y), but are rotated through a certain angle θ , then the elasticity matrix of the L th lamina can be determined using the following transformation rules

$$\begin{aligned} \sigma_{1,2,3} &= \mathbf{T} \sigma_{x,y,z} \\ \epsilon_{1,2,3} &= \mathbf{T}' \epsilon_{x,y,z}; \end{aligned} \tag{6d}$$

where

$$\mathbf{T} = \begin{bmatrix} \mathbf{T}_1 & \mathbf{0} \\ \mathbf{0} & \mathbf{T}_2 \end{bmatrix} \quad \text{and} \quad \mathbf{T}' = \begin{bmatrix} \mathbf{T}'_1 & \mathbf{0} \\ \mathbf{0} & \mathbf{T}'_2 \end{bmatrix}$$

$$\begin{bmatrix} \sigma_1 \\ \sigma_2 \\ \tau_{12} \\ \tau_{13} \\ \tau_{23} \end{bmatrix}^L = \begin{bmatrix} C_{11} & C_{12} & 0 & 0 & 0 \\ & C_{22} & 0 & 0 & 0 \\ & & C_{33} & 0 & 0 \\ \text{Symmetric} & & & C_{44} & 0 \\ & & & & C_{55} \end{bmatrix}^L \begin{bmatrix} \epsilon_1 \\ \epsilon_2 \\ \gamma_{12} \\ \gamma_{13} \\ \gamma_{23} \end{bmatrix}^L \tag{6a}$$

or symbolically

$$\sigma_{1,2,3}^L = \mathbf{C}^L \epsilon_{1,2,3}^L. \tag{6b}$$

where $\sigma'_{1,2,3} = (\sigma_1, \sigma_2, \tau_{12}, \tau_{13}, \tau_{23})$ is the stress component vector, $\epsilon'_{1,2,3} = (\epsilon_1, \epsilon_2, \gamma_{12}, \gamma_{13}, \gamma_{23})$ is the physical strain component vector referred to the lamina coordinates (1, 2, 3) as shown in Fig. 1 and the $C_{i,j}$ s are the elements of the composite material stiffness matrix giving the stress-strain relations of L th lamina in the lamina axes (1, 2, 3) and these are defined as follows:

$$\begin{aligned} C_{11} &= \left(\frac{E_1}{1 - \nu_{12} \nu_{21}} \right); \\ C_{12} &= \left(\frac{\nu_{12} E_2}{1 - \nu_{12} \nu_{21}} \right); \end{aligned}$$

in which

$$\begin{aligned} \mathbf{T}_1 &= \begin{bmatrix} c^2 & s^2 & 2sc \\ s^2 & c^2 & -2sc \\ -sc & sc & c^2 - s^2 \end{bmatrix}; \\ \mathbf{T}'_1 &= \begin{bmatrix} c^2 & s^2 & sc \\ s^2 & c^2 & -sc \\ -2sc & 2sc & c^2 - s^2 \end{bmatrix}; \end{aligned}$$

and

$$\mathbf{T}_2 = \begin{bmatrix} c & s \\ -s & c \end{bmatrix}, \tag{6e}$$

where $c = \cos \theta$, $s = \sin \theta$ and $\mathbf{T}^{-1} = \mathbf{T}'$.

The stress-strain relations of the L th lamina in the laminate coordinate axes (x, y, z) can then be written as,

$$\bar{\sigma}_{x,y,z} = (\mathbf{T}^{-1} \cdot \mathbf{C} \cdot \mathbf{T}') \bar{\epsilon}_{x,y,z} \tag{6f}$$

or

$$\bar{\sigma}_{x,y,z} = Q\bar{\epsilon}_{x,y,z} \quad \text{with} \quad Q = \mathbf{T}^{-1} \cdot \mathbf{C} \cdot \mathbf{T} \quad (6g)$$

and in the expanded form as

$$\begin{bmatrix} \sigma_x \\ \sigma_y \\ \tau_{xy} \\ \tau_{xz} \\ \tau_{yz} \end{bmatrix}^L = \begin{bmatrix} Q_{11} & Q_{12} & Q_{13} & 0 & 0 \\ & Q_{22} & Q_{23} & 0 & 0 \\ & & Q_{33} & 0 & 0 \\ \text{Symmetric} & & & Q_{44} & Q_{45} \\ & & & & Q_{55} \end{bmatrix}^L \begin{bmatrix} \epsilon_x \\ \epsilon_y \\ \gamma_{xy} \\ \gamma_{xz} \\ \gamma_{yz} \end{bmatrix}^L \quad (6h)$$

in which $\sigma'_{x,y,z} = (\sigma_x, \sigma_y, \tau_{xy}, \tau_{xz}, \tau_{yz})$ is the stress vector, $\epsilon'_{x,y,z} = (\epsilon_x, \epsilon_y, \gamma_{xy}, \gamma_{xz}, \gamma_{yz})$ is the strain vector with respect to the shell axes and the matrix Q gives the stress and strain relations of the L th lamina in the shell axes and its elements can be written explicitly as follows:

$$\begin{aligned} Q_{11} &= C_{11} \cdot c^4 + (2 \cdot C_{12} + 4 \cdot C_{33}) \cdot s^2 \cdot c^2 + C_{22} \cdot s^4 \\ Q_{12} &= C_{12} \cdot (c^4 + s^4) + (C_{11} + C_{22} - 4 \cdot C_{33}) \cdot s^2 \cdot c^2 \\ Q_{13} &= (C_{11} - C_{12} - 2 \cdot C_{33}) \cdot s \cdot c^3 \\ &\quad + (C_{12} - C_{22} + 2 \cdot C_{33}) \cdot s^3 \cdot c \\ Q_{22} &= C_{11} \cdot s^4 + (2 \cdot C_{12} + 4 \cdot C_{33}) \cdot s^2 \cdot c^2 + C_{22} \cdot c^4 \\ Q_{23} &= (C_{11} - C_{12} - 2 \cdot C_{33}) \cdot s^3 \cdot c \\ &\quad + (C_{12} - C_{22} + 2 \cdot C_{33}) \cdot s \cdot c^3 \\ Q_{33} &= C_{33} \cdot (c^4 + s^4) + (C_{11} - 2 \cdot C_{12} \\ &\quad + C_{22} - 2 \cdot C_{33}) \cdot s^2 \cdot c^2 \\ Q_{44} &= C_{44} \cdot c^2 + C_{55} \cdot s^2 \\ Q_{45} &= (C_{44} - C_{55}) \cdot c \cdot s \\ Q_{55} &= C_{44} \cdot s^2 + C_{55} \cdot c^2. \end{aligned} \quad (6i)$$

By substituting the expressions for the strain components in eqn (5) while carrying out the explicit integration of the through the shell thickness leads to the definition of the stress resultant vector $\bar{\sigma}$ which can be written as follows (see Kant and Kommineni [19]):

$$\begin{aligned} \bar{\sigma}' &= (N_x, N_y, N_{xy}, N_x^*, N_y^*, N_{xy}^*, \\ &\quad M_x, M_y, M_{xy}, M_x^*, M_y^*, M_{xy}^*, \\ &\quad Q_x, Q_y, Q_x^*, Q_y^*, S_x, S_y, S_x^*, S_y^*), \end{aligned} \quad (7a)$$

in which

$$\begin{aligned} \begin{bmatrix} N_x & N_x^* \\ N_y & N_y^* \\ N_{xy} & N_{xy}^* \end{bmatrix} &= \sum_{L=1}^{NL} \int_{z_L}^{z_{L+1}} \begin{bmatrix} \sigma_x \\ \sigma_y \\ \tau_{xy} \end{bmatrix} [1, z^2] dz \\ \begin{bmatrix} M_x & M_x^* \\ M_y & M_y^* \\ M_{xy} & M_{xy}^* \end{bmatrix} &= \sum_{L=1}^{NL} \int_{z_L}^{z_{L+1}} \begin{bmatrix} \sigma_x \\ \sigma_y \\ \tau_{xy} \end{bmatrix} [z, z^3] dz \\ \begin{bmatrix} Q_x & Q_x^* & S_x & S_x^* \\ Q_y & Q_y^* & S_y & S_y^* \end{bmatrix} &= \sum_{L=1}^{NL} \int_{z_L}^{z_{L+1}} \begin{bmatrix} \tau_{xz} \\ \tau_{yz} \end{bmatrix} [1, z^2, z, z^3] dz. \end{aligned} \quad (7b)$$

After integration these relations can be written in matrix form, which defines the stress resultant and mid-surface strain relations of the laminated shell and is given by

$$\begin{bmatrix} \mathbf{N} \\ \mathbf{M} \\ \mathbf{Q} \end{bmatrix} = \begin{bmatrix} \mathbf{D}_m & \mathbf{D}_c & \mathbf{0} \\ \mathbf{D}'_c & \mathbf{D}_b & \mathbf{0} \\ \mathbf{0} & \mathbf{0} & \mathbf{D}_s \end{bmatrix} \begin{bmatrix} \bar{\epsilon}_m \\ \bar{\epsilon}_b \\ \bar{\epsilon}_s \end{bmatrix} \quad (8a)$$

or symbolically

$$\bar{\sigma} = \mathbf{D}\bar{\epsilon} \quad (8b)$$

where

$$\begin{aligned} \mathbf{N}' &= [N_x, N_y, N_{xy}, N_x^*, N_y^*, N_{xy}^*] \\ \mathbf{M}' &= [M_x, M_y, M_{xy}, M_x^*, M_y^*, M_{xy}^*] \\ \mathbf{Q}' &= [Q_x, Q_y, Q_x^*, Q_y^*, S_x, S_y, S_x^*, S_y^*] \\ \bar{\sigma}' &= [N_x, N_y, N_{xy}, N_x^*, N_y^*, N_{xy}^*, M_x, M_y, \\ &\quad M_{xy}, M_x^*, M_y^*, M_{xy}^*, Q_x, Q_y, \\ &\quad Q_x^*, Q_y^*, S_x, S_y, S_x^*, S_y^*] \end{aligned} \quad (8c)$$

and the stiffness coefficient matrices \mathbf{D}_m , \mathbf{D}_c , \mathbf{D}_b and \mathbf{D}_s , corresponding to the membrane, the coupling between the membrane and bending, the bending and shear deformations, respectively are defined as follows:

$$\begin{aligned} \mathbf{D}_m &= \sum_{L=1}^{NL} \begin{bmatrix} \mathbf{Q}_{ij} H_1 & \mathbf{Q}_{ij} H_3 \\ \mathbf{Q}_{ij} H_3 & \mathbf{Q}_{ij} H_5 \end{bmatrix}, \\ \mathbf{D}_c &= \sum_{L=1}^{NL} \begin{bmatrix} \mathbf{Q}_{ij} H_2 & \mathbf{Q}_{ij} H_4 \\ \mathbf{Q}_{ij} H_4 & \mathbf{Q}_{ij} H_6 \end{bmatrix}, \\ \mathbf{D}_b &= \sum_{L=1}^{NL} \begin{bmatrix} \mathbf{Q}_{ij} H_3 & \mathbf{Q}_{ij} H_5 \\ \mathbf{Q}_{ij} H_5 & \mathbf{Q}_{ij} H_7 \end{bmatrix}, \\ \mathbf{D}_s &= \sum_{L=1}^{NL} \begin{bmatrix} \mathbf{Q}_{lm} H_1 & \mathbf{Q}_{lm} H_3 & \mathbf{Q}_{lm} H_2 & \mathbf{Q}_{lm} H_4 \\ \mathbf{Q}_{ij} H_3 & \mathbf{Q}_{ij} H_5 & \mathbf{Q}_{lm} H_4 & \mathbf{Q}_{lm} H_6 \\ \mathbf{Q}_{lm} H_2 & \mathbf{Q}_{lm} H_4 & \mathbf{Q}_{lm} H_3 & \mathbf{Q}_{lm} H_5 \\ \mathbf{Q}_{lm} H_4 & \mathbf{Q}_{lm} H_6 & \mathbf{Q}_{lm} H_5 & \mathbf{Q}_{lm} H_7 \end{bmatrix}. \end{aligned} \tag{8d}$$

In the above relations $i, j = 1, 2, 3$ and $l, m = 4, 5$

$$H_k = \frac{1}{k} (z_{L+1}^k - z_L^k), \quad k = 1, 2, 3, 4, 5, 6, 7.$$

NL is the number of layers and $\bar{\epsilon} = (\bar{\epsilon}'_m, \bar{\epsilon}'_b, \bar{\epsilon}'_s)'$ represents the mid-surface membrane, bending and shear strain components respectively and are defined as follows:

$$\bar{\epsilon}_m = \begin{bmatrix} \frac{\partial u_o}{\partial x} + \frac{w_o}{R_1} + \frac{1}{2} \left(\frac{\partial w_o}{\partial x} \right)^2 \\ \frac{\partial v_o}{\partial y} + \frac{w_o}{R_2} + \frac{1}{2} \left(\frac{\partial w_o}{\partial y} \right)^2 \\ \frac{\partial v_o}{\partial x} + \frac{\partial u_o}{\partial y} + \frac{\partial w_o}{\partial x} \frac{\partial w_o}{\partial y} \\ \frac{\partial u_o^*}{\partial x} \\ \frac{\partial v_o^*}{\partial y} \\ \frac{\partial v_o^*}{\partial x} + \frac{\partial u_o^*}{\partial y} \end{bmatrix};$$

$$\bar{\epsilon}_b = \begin{bmatrix} \frac{\partial \theta_\gamma}{\partial x} \\ \frac{\partial \theta_\gamma}{\partial y} \\ \frac{\partial \theta_\gamma}{\partial x} + \frac{\partial \theta_\gamma}{\partial y} \\ \frac{\partial \theta_\gamma^*}{\partial x} \\ \frac{\partial \theta_\gamma^*}{\partial y} \\ \frac{\partial \theta_\gamma^*}{\partial x} + \frac{\partial \theta_\gamma^*}{\partial y} \end{bmatrix};$$

$$\bar{\epsilon}_s = \begin{bmatrix} \theta_\gamma + \frac{\partial w_o}{\partial x} - \frac{u_o}{R_1} \\ \theta_\gamma + \frac{\partial w_o}{\partial y} - \frac{v_o}{R_2} \\ 3\theta_\gamma^* - \frac{u_o^*}{R_1} \\ 3\theta_\gamma^* - \frac{v_o^*}{R_2} \\ 2u_o^* - \frac{\theta_\gamma}{R_1} \\ 2v_o^* - \frac{\theta_\gamma}{R_2} \\ -\frac{\theta_\gamma^*}{R_1} \\ -\frac{\theta_\gamma^*}{R_2} \end{bmatrix}. \tag{8e}$$

C⁰ FINITE ELEMENT FORMULATION

The finite element used here is a nine-noded isoparametric quadrilateral element. The laminate displacement field in the element can be expressed in terms of nodal variables, such that:

$$\mathbf{d}(\xi, \eta) = \sum_{i=1}^{NN} N_i(\xi, \eta) \cdot \mathbf{d}_i, \tag{9}$$

where NN represents number of nodes in the element, $N_i(\xi, \eta)$ defines the interpolation function associated with node i in terms of normalized coordinates ξ, η and \mathbf{d}_i is generalized mid-surface displacement vector at node i , such that

$$\mathbf{d}_i = (u_{oi}, v_{oi}, w_{oi}, \theta_{\gamma i}, u_{oi}^*, v_{oi}^*, \theta_{\gamma i}^*, \theta_{\gamma i}^*). \tag{10}$$

The generalized vectors of the mid-surface strain and its variation $\bar{\epsilon}$ and $\delta \bar{\epsilon}$ respectively, are written in terms of nodal displacements \mathbf{a} such that, $\mathbf{a}' = (\mathbf{d}'_1, \mathbf{d}'_2, \mathbf{d}'_3, \dots, \mathbf{d}'_{NN})$, displacement gradient θ_{nl} and cartesian derivatives of shape functions (see Zienkiewicz [32])

$$\begin{aligned} \bar{\epsilon} &= (\mathbf{B}_o + \frac{1}{2} \cdot \mathbf{B}_{nl}) \cdot \mathbf{a} \\ \delta \bar{\epsilon} &= (\mathbf{B}_o + \mathbf{B}^{nl}) \cdot \delta \mathbf{a} \\ \delta \bar{\epsilon} &= \sum_{i=1}^{NN} \mathbf{B}_i \cdot \delta \mathbf{d}_i = \mathbf{B} \cdot \delta \mathbf{a} \\ \delta \bar{\sigma} &= \mathbf{D} \cdot \mathbf{B} \cdot \delta \mathbf{a}, \end{aligned} \tag{11}$$

where \mathbf{B}_o is the linear strain-displacement matrix and \mathbf{B}_{nl} the non-linear strain-displacement matrix which is linearly dependent upon the nodal displacement \mathbf{a} . \mathbf{B} is the total strain-displacement matrix and the non-zero elements of the \mathbf{B} matrix corresponding to the membrane, flexure and shear terms are as follows.

Membrane and flexure terms (size of matrix, 12×9):

$$\begin{aligned}
 B_{1,1} &= B_{3,2} = B_{4,6} = B_{6,7} = B_{7,4} = B_{9,5} = B_{10,8} \\
 &= B_{12,9} = \frac{\partial N_i}{\partial x} \\
 B_{2,2} &= B_{3,1} = B_{5,7} = B_{6,6} = B_{8,5} = B_{9,4} \\
 &= B_{11,9} = B_{12,8} = \frac{\partial N_i}{\partial y} \\
 B_{1,3} &= \frac{N_i}{R_1} + \frac{\partial w_o}{\partial x} \cdot \frac{\partial N_i}{\partial x} \\
 B_{2,3} &= \frac{N_i}{R_1} + \frac{\partial w_o}{\partial y} \cdot \frac{\partial N_i}{\partial y} \\
 B_{3,3} &= \frac{\partial w_o}{\partial x} \cdot \frac{\partial N_i}{\partial y} + \frac{\partial w_o}{\partial y} \cdot \frac{\partial N_i}{\partial x}
 \end{aligned} \tag{12}$$

Shear terms (size of matrix, 8×9):

$$\begin{aligned}
 B_{1,3} &= \frac{\partial N_i}{\partial x}; \quad B_{2,3} = \frac{\partial N_i}{\partial y}; \quad B_{1,4} = B_{2,5} = N_i; \\
 B_{3,8} &= B_{4,9} = 3N_i; \quad B_{5,6} = B_{6,7} = 2N_i \\
 B_{1,1} &= B_{3,6} = B_{5,4} = B_{7,8} = -\frac{N_i}{R_1}; \\
 B_{2,2} &= B_{4,7} = B_{6,5} = B_{8,9} = -\frac{N_i}{R_2}
 \end{aligned} \tag{13}$$

The discrete expressions for the variation of strain energy, kinetic energy and work done by the external loads in eqn (5b) are as follows

$$\begin{aligned}
 \delta U &= \delta \mathbf{a}' \left(\int_A \mathbf{B}' \bar{\boldsymbol{\sigma}} \, dx \, dy \right) \\
 \delta E &= -\delta \mathbf{a}' \left(\int_A \mathbf{N}' \bar{\mathbf{m}} \mathbf{N} \, dx \, dy \right) \cdot \ddot{\mathbf{a}} \\
 \delta W &= \delta \mathbf{a}' \left(\int_A \mathbf{N}' \mathbf{q}_o \, dx \, dy \right),
 \end{aligned} \tag{14}$$

where \mathbf{a} , $\ddot{\mathbf{a}}$ and \mathbf{q}_o respectively define the nodal displacement, acceleration and load vectors. \mathbf{N} is defined as the shape function matrix, i.e. $(\mathbf{N}_1, \mathbf{N}_2, \dots, \mathbf{N}_{NN})$. Substituting eqn (14) in eqn (5b) and simplifying the equation we get

$$\int_{t_1}^{t_2} \delta \mathbf{a}' [\mathbf{M} \ddot{\mathbf{a}} + \mathbf{P}(a, t) - \mathbf{F}(t)] \, dt = 0. \tag{15}$$

Since this relation is valid for every virtual displacement $\delta \mathbf{a}$, we have

$$\mathbf{M} \ddot{\mathbf{a}} + \mathbf{P}(a, t) = \mathbf{F}(t), \tag{16}$$

which is the global equation of motion, where \mathbf{M} is the global mass matrix, $\mathbf{P}(a, t)$ and $\mathbf{F}(t)$ are respectively the global internal and external load vectors which are defined as

$$\mathbf{P}(a, t) = \int_A \mathbf{B}' \bar{\boldsymbol{\sigma}} \, dx \, dy \tag{17a}$$

$$\mathbf{F}(t) = \int_A \mathbf{N}' \mathbf{q}_o \, dx \, dy. \tag{17b}$$

SPECIAL MASS MATRIX DIAGONALIZATION SCHEME

The inertia force vector requires the evaluation of the mass matrix \mathbf{M} . This consistent mass matrix is not diagonal and it must therefore be diagonalized in some way if it is to be useful in the explicit time marching scheme. For the quadratic isoparametric element used here, several alternatives were investigated by Hinton *et al.* [33]. For the sake of completeness, the most efficient scheme found by them is summarized below for ready reference.

(i) Only the diagonal coefficients of the consistent mass matrix are computed

$$\mathbf{M} = \int_A \mathbf{N}' \bar{\mathbf{m}} \mathbf{N} \, dA, \tag{18}$$

where

$$\bar{\mathbf{m}} = \begin{bmatrix} I_1 & & & & & & & & 0 \\ & I_1 & & & & & & & \\ & & I_1 & & & & & & \\ & & & I_2 & & & & & \\ & & & & I_2 & & & & \\ & & & & & I_3 & & & \\ & & & & & & I_3 & & \\ & & & & & & & I_4 & \\ 0 & & & & & & & & I_4 \end{bmatrix}$$

in which I_1, I_2, I_3 and I_4 are normal inertia, rotary inertia and higher order inertia terms respectively. These are as follows:

$$(I_1, I_2, I_3, I_4) = \sum_{L=1}^{NL} \int_{-z_L}^{z_{L+1}} (1, z^2, z^4, z^6) \rho^L \, dz$$

and ρ^L is material density of the L th layer.

(ii) The total mass of the element is computed

$$M_i = \int_V \rho \, dv. \tag{19}$$

(iii) The diagonal coefficients M_{ii} associated with a particular translation (but not rotation) degree of freedom, are summed such that

$$\text{SUM} = \sum M_{ii}. \quad (20)$$

(iv) All the diagonal coefficients of the consistent mass matrix are scaled in the following manner such that the total mass of the element is conserved:

$$M_{ii}^d = M_{ii} \cdot \frac{M_i}{\text{SUM}}. \quad (21)$$

SOLUTION ALGORITHM

The numerical solution to the ordinary differential equation (16) is obtained using an explicit central difference scheme. The advantage of using the central difference method should now become apparent. Since no internal force vector and mass matrices of the complete element assemblage need to be calculated, the solution can essentially be carried out on the element level and relatively little high speed storage is required. Since the mass matrix \mathbf{M} is a diagonal matrix, the set of equations (16) are uncoupled to give new displacement values without requiring the matrix factorization. Further, the usual iterative solution procedure for the solution of a non-linear system of equations is completely avoided since the solution in the time domain is obtained here for each degree of freedom independently. Using the central difference scheme, systems of very large order equations can be solved efficiently.

Equation (16) can be written in a scalar form as:

$$m_i \ddot{a}_i + p_i = f_i, \quad (22a)$$

where subscript i denotes the i th degree of freedom and the other symbols have their usual meanings.

In the explicit time marching scheme used here the velocities and accelerations are approximated using the central difference formulae as:

$$\begin{aligned} \dot{a}_i^n &= (a_i^{n+1} - a_i^{n-1})/2 \cdot \Delta t \\ \ddot{a}_i^n &= (a_i^{n+1} - 2 \cdot a_i^n + a_i^{n-1})/\Delta t^2, \end{aligned} \quad (22b)$$

where $n-1$, n and $n+1$ denote three successive time stations and Δt is the time step length. Using the above approximation, eqn (22a) can be rewritten as:

$$m_i \cdot (a_i^{n+1} - 2 \cdot a_i^n + a_i^{n-1})/\Delta t^2 + p_i^n - f_i^n = 0 \quad (22c)$$

It becomes clear that the values of a_i^{n+1} can be determined from the two previous displacement, a_i^n and a_i^{n-1} by rewriting eqn (22c)

$$a_i^{n+1} = \left(\frac{\Delta t^2}{m_i} \right) \cdot (-p_i^n + f_i^n) - a_i^{n-1} + 2 \cdot a_i^n. \quad (22d)$$

If the values a_i^0 and \dot{a}_i^0 are the specified initial displacement and velocity conditions, then a special starting algorithm can be established as follows,

$$\dot{a}_i^0 = (a_i^1 - a_i^{-1})/2 \cdot \Delta t \quad (22e)$$

$$a_i^{-1} = a_i^1 - 2\Delta t \dot{a}_i^0 \quad (22f)$$

$$a_i^1 = a_i^0 + \Delta t \dot{a}_i^0 + \Delta t^2(-p_i^0 + f_i^0)/2m_i. \quad (22g)$$

This stepping scheme (22d) for $n = 1, 2, 3, \dots$, along with a starting algorithm (22g), are used to carry out in a straightforward manner the time history analysis of the non-linear system.

Since there is no estimate on the time step for the non-linear analysis available in the literature, in the present investigation the initial estimate is calculated using the modified form of Tsui and Tong [34] by Kant and Mallikarjuna [25]

$$\begin{aligned} \Delta t &\leq \Delta r_{crit} \\ &= \Delta x \left(\frac{\rho(1-\nu^2)/E_2 R}{\{2 + (1-\nu)(\pi^2/12)(1 + 1.5(\Delta x/h)^2)\}} \right)^{1/2} \end{aligned} \quad (23)$$

in which Δx is the smallest distance between adjacent nodes in any quadrilateral element used. E_1 and E_2 are the Young's moduli in the 1 and 2 directions respectively (see Fig. 1) and $R = E_1/E_2$. The final estimate is done after carrying out convergence checks in order to save computational costs.

NUMERICAL RESULTS

In the present study a nine node quadrilateral isoparametric element is employed. Due to the biaxial symmetry of the problems discussed only one quadrant of the laminated shell is analysed with a 2×2 mesh except for angle-ply laminated shells which are analysed by considering full laminates with a 4×4 mesh. These discretizations were established by an extensive convergence study [19-27]. In all the numerical computations, the selective integration rule is employed. A 3×3 Gaussian rule is used to compute the membrane, the coupling between the membrane and bending and bending deformations, while a 2×2 rule is used to evaluate the terms associated with transverse shear deformation. The element mass matrix is evaluated using a 3×3 Gauss-quadrature rule. For numerical computations, two programs, viz., a first order shear deformation theory (FOST5) and a higher order shear deformation theory (HOST9) with five and nine degrees of freedom per node respectively are developed. All the computations were carried out in single precision on CDC Cyber 180/840 computer with sixteen significant digits word-length at the Indian Institute of Technology, Bombay, India. All the stress values are evaluated at the Gauss points and these are reported nearest to

Table 1. Boundary conditions

| Type | $x = 0/x = a$ | $x = a/2$ | $y = 0/y = b$ | $y = b/2$ |
|------|----------------|----------------|----------------|----------------|
| S | $v_o = 0$ | $u_o = 0$ | $u_o = 0$ | $v_o = 0$ |
| | $\theta_x = 0$ | $\theta_x = 0$ | $\theta_x = 0$ | $\theta_x = 0$ |
| | $w_o = 0$ | | $w_o = 0$ | |
| C | $u_o = 0$ | $u_o = 0$ | $u_o = 0$ | |
| | $v_o = 0$ | $v_o = 0$ | $v_o = 0$ | $v_o = 0$ |
| | $\theta_x = 0$ | $\theta_x = 0$ | $\theta_x = 0$ | $\theta_x = 0$ |
| | $\theta_y = 0$ | $\theta_y = 0$ | $\theta_y = 0$ | $\theta_y = 0$ |
| | $w_o = 0$ | | $w_o = 0$ | |

their maximum value locations. A shear correction coefficient of 5/6 is used in the first order shear deformation theory (FOST). For historical reasons, the present results are compared with the available results which are based on material properties which do not satisfy the symmetry condition (see, e.g., [8, 18], that is $v_{12}/E_1 \neq v_{21}/E_2$).

In order to test the accuracy and efficiency of the developed algorithm, and to investigate the effects of transverse shear deformations, the following material property sets were used in obtaining the numerical results.

Material set 1: The material properties are taken from [18]: $E_1 = 19.2 \times 10^6$ psi; $E_2 = 1.56 \times 10^6$ psi; $G_{12} = G_{13} = 0.82 \times 10^6$ psi; $G_{23} = 0.523 \times 10^6$ psi; $\rho = 0.00012$ lb s²/in⁴; $v_{12} = v_{21} = 0.24$.

Material set 2: The material properties are taken from [8]: $E_1 = 25 E_2$, $G_{12} = G_{13} = 0.5E_2$; $G_{23} = 0.2E_2$; $v_{12} = v_{21} = 0.25$; $E_2 = 10^6$ N/cm²; $\rho = 1$ N s²/cm⁴; $a = b = 100$ cm; $h = 1$ cm; $R_1 = R_2 = 1000$ cm and $q = 1$ N/cm².

Material set 3: The material properties are taken from [8]: $E_1 = 7.5 \times 10^6$ psi; $E_2 = 2 \times 10^6$ psi; $G_{12} = G_{23} = G_{31} = 1.25 \times 10^6$ psi; $v_{12} = v_{21} = 0.25$; $\rho = 1$ lb s²/in⁴; $l = 20$ in; $h = 1$ in; $R = 20$ in.

Material set 4. The material properties are taken from [8, 35]: Geometry $R_1 = R_2 = 100$, $a = b = 20$.

Material properties: face sheet properties the same as material set 1. Thickness of each face sheet = $0.1h$. Core properties: Thickness of core = $0.8h$.

$$G_{23} = 5.17 \times 10^4 \text{ psi, } G_{13} = 1.344 \times 10^5 \text{ psi;}$$

$$\rho = 0.1242 \times 10^{-5} \text{ lb s}^2/\text{in}^4.$$

Material set 5: The material properties are taken from [29, 35]: $a = b = 320$ in; $h = 32$ in; $R = 960$ in. Isotropic facings: thickness of each facing = $0.1h$.

$$E = 0.6895 \times 10^7 \text{ psi; } \nu = 0.33;$$

$$\rho = 2.821 \times 10^{-5} \text{ lb s}^2/\text{in}^4.$$

Thickness of core = $0.8h$; $\rho = 0.1242 \times 10^{-5}$ lb s²/in⁴.

Core 1: $G_{23} = 5.17 \times 10^4$ psi; $G_{13} = 1.344 \times 10^5$ psi

Core 2: $G_{23} = 5.17 \times 10^3$ psi; $G_{13} = 1.344 \times 10^4$ psi

Core 3: $G_{23} = 5.17 \times 10^2$ psi; $G_{13} = 1.344 \times 10^3$ psi.

The finite element displacement formulation developed in this paper is based entirely on assumed displacement functions and thus only displacement boundary conditions can be enforced. The boundary conditions corresponding to the present higher order formulation are specified in Table 1, for a simple support (S) and a clamped (C) boundaries.

The corresponding boundary conditions for the first order shear deformation theory is simply obtained by omitting the higher order starred (*) displacement quantities. For example there are nine displacement quantities required to be specified at $x = 0, a$ for a clamped (C) types of boundary condition in this higher order formulation (HOST), whereas in the first order formulation (FOST) the corresponding boundary conditions should be only five. The simple support (S) boundary condition has been especially chosen in order to compare our results with those of other authors. The edge conditions, which have been derived in a variationally consistent manner in the present higher order theory may not appear so (except in the case of fully clamped edge specified by C), because, in any case, the natural boundary conditions can not be prescribed in the displacement based finite element method.

The following results are grouped into two categories, viz., linear analysis and non-linear analysis.

Linear analysis

1. An unsymmetric cross-ply laminate. A simply supported cross-ply (0°/90°) spherical shell with $a = b = 20$ in, $h = 2$ in, $R = 5a$ and the material properties as per material set 1 subjected to a sinusoidally distributed load of maximum intensity $q_o = 2000$ psi and in the time domain, both sinusoidal and triangular pulses of duration $t_o = 0.003$ sec, i.e.,

$$F(t) = \sin\left(\frac{\pi t}{t_o}\right) \quad 0 < t < t_o: \text{ sinusoidal pulse}$$

$$F(t) = 0 \quad t > t_o \quad (24a)$$

$$F(t) = \left(1 - \frac{t}{t_o}\right) \quad 0 < t < t_o: \text{ triangular pulse}$$

$$F(t) = 0 \quad t > t_o \quad (24b)$$

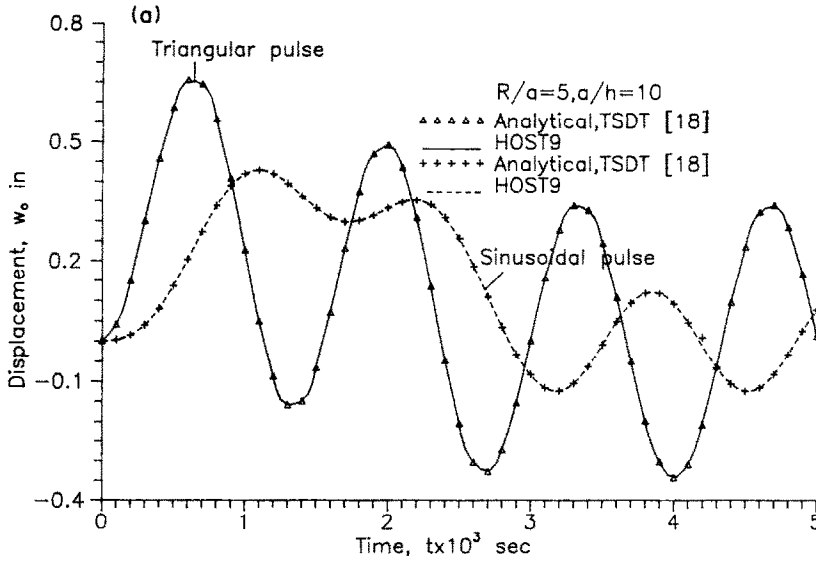


Fig. 2(a). Displacement vs time for a simply supported cross-ply (0°/90°) spherical shell subjected to a sinusoidal transverse load ($q_0 = 2000$ psi, $t_0 = 0.003$ sec, $\Delta t = 2.5 \mu$ sec).

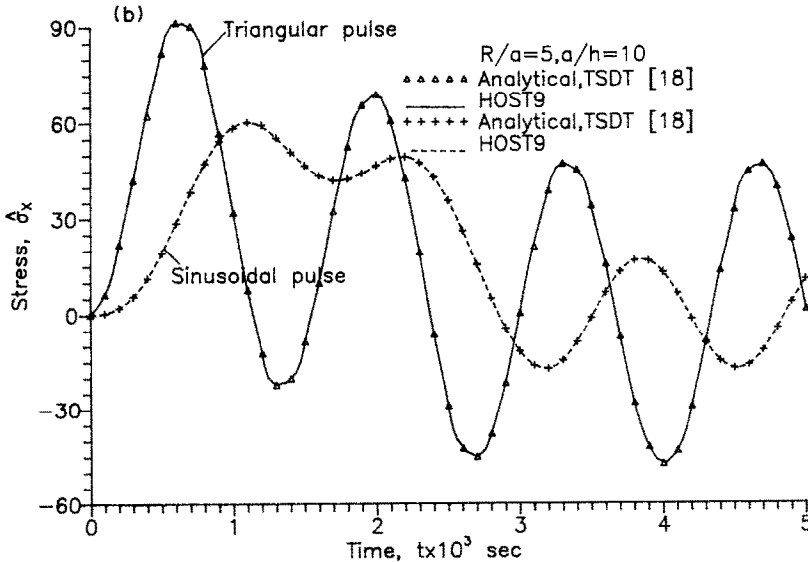


Fig. 2(b). Stress vs time for a simply supported cross-ply (0°/90°) spherical shell subjected to a sinusoidal transverse load ($q_0 = 2000$ psi, $t_0 = 0.003$ sec, $\Delta t = 2.5 \mu$ sec).

are considered. The non-dimensional quantity used for representing the stress is

$$\hat{\sigma}_x = \sigma_x(a/2, b/2, h/2)/q_0. \quad (25)$$

The present higher order results for central displacement and stress variations with respect to time are compared with closed-form two dimensional solutions which are based on a higher order shear deformation theory and is presented by Reddy and Khdeir [18]. The results are plotted in Figs 2(a) and 2(b). The present results match exactly the closed-form solutions of a third order theory given by Reddy and Khdeir [18].

2. *Symmetric cross-ply laminate.* A simply supported cross-ply (0°/90°/0°) spherical shell with the geometry, material properties, loading and non-dimensional quantities the same as used in the previous problem is considered. The present higher order results for the variation of central displacement and stress with respect to time are compared with the analytical higher order solutions given by Reddy and Khdeir [18] and are plotted in Figs 3(a) and (b).

From these results, the following observations are made:

- The present results match exactly the closed-form two dimensional solutions based on a higher order shear deformation theory for both symmetric and unsymmetric laminated shells.

- The response due to the triangular pulse has a larger amplitude than that due to the sinusoidal pulse.
- The symmetric cross-ply laminate is stiffer than the corresponding unsymmetric laminate.

The foregoing evaluations established the validity of the present C^0 finite element higher order formulation in linear analysis.

Non-linear analysis

1. *Cantilever beam under uniform load.* A cantilever beam of length 10 in, width 1 in, thickness 1 in,

modulus of elasticity 1.2×10^4 psi, Poisson's ratio 0.2 and density 10^{-6} lb s²/in⁴ is analysed using a 2×2 mesh of nine node elements in the half width of the beam. The load is assumed to be a step load (i.e., applied at time $t = 0$ and kept indefinitely) of intensity 2.85 lb/in². The present results for the variation of the tip displacement with respect to time are compared with Bathe *et al.* [36], who used a fully non-linear model derived from three dimensional elasticity theory. The results are presented in Fig. 4. The difference in results at peak amplitude is partly due to the fact that the load is treated as conservative in the present analysis whereas it is treated as non-conservative by Bathe *et al.* [36].

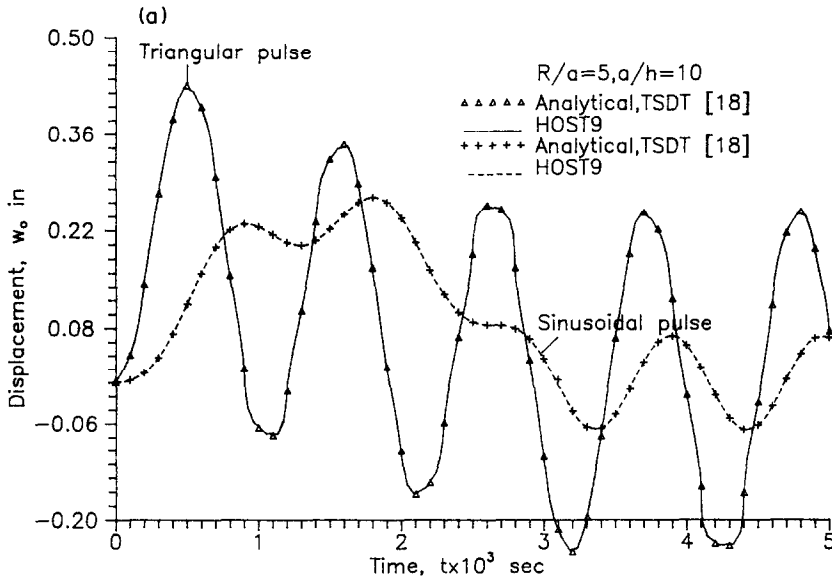


Fig. 3(a). Displacement vs time for a simply supported cross-ply ($0^\circ/90^\circ/0^\circ$) spherical shell subjected to a sinusoidal transverse load ($q_0 = 2000$ psi, $t_0 = 0.003$ sec, $\Delta t = 2.5 \mu$ sec).

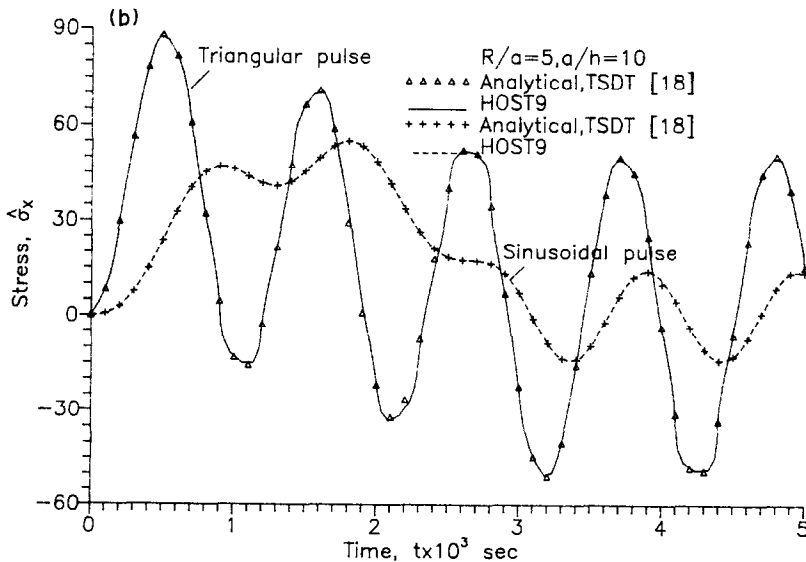


Fig. 3(b). Stress vs time for a simply supported cross-ply ($0^\circ/90^\circ/0^\circ$) spherical shell subjected to a sinusoidal transverse load ($q_0 = 2000$ psi, $t_0 = 0.003$ sec, $\Delta t = 2.5 \mu$ sec).

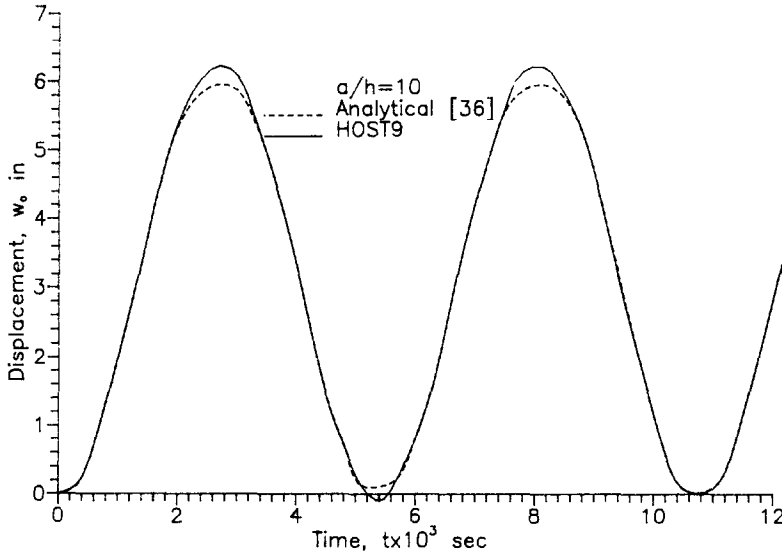


Fig. 4. Displacement vs time for a cantilever beam subjected to a uniform transverse load ($q_0 = 2.85 \text{ lb/in}^2, \Delta t = 0.675 \mu\text{sec}$).

2. *An unsymmetric cross-ply spherical shell.* A simply supported cross-ply ($0^\circ/90^\circ$) spherical shell geometry, material properties and loading as per material set 2 subjected to a uniform external pressure load is considered. The present results are compared with Reddy and Chandrashekhara [8] and are plotted in Fig. 5. The non-dimensional quantity used for representing the displacement is defined as

$$\hat{w}_0 = \frac{w_0}{q_0} \quad (26)$$

It is observed that as the intensity of the load increases the period of vibration as well as the peak amplitude increase.

3. *A cylindrical shell.* A clamped cross-ply ($0^\circ/90^\circ$) cylindrical shell with geometry and material properties as per material set 3 subjected to an internal uniform step pulse (i.e., applied at time $t = 0$ and kept indefinitely) of intensity $q_0 = 5000 \text{ psi}$ is considered. The present results for the displacement are compared with Reddy and Chandrashekhara [8] and are plotted in Fig. 6. The present results match exactly those of Reddy and Chandrashekhara [8]. This shows the correctness and reliability of the present formulation for cylindrical shells.

4. *An angle-ply spherical shell.* A simply supported angle-ply ($\theta^\circ/-\theta^\circ/\theta^\circ$) for $\theta = 30^\circ, 45^\circ, 60^\circ, 75^\circ$ with $R/a = 5, a/h = 10$ and the material properties as per material set 1 subjected to a triangular time

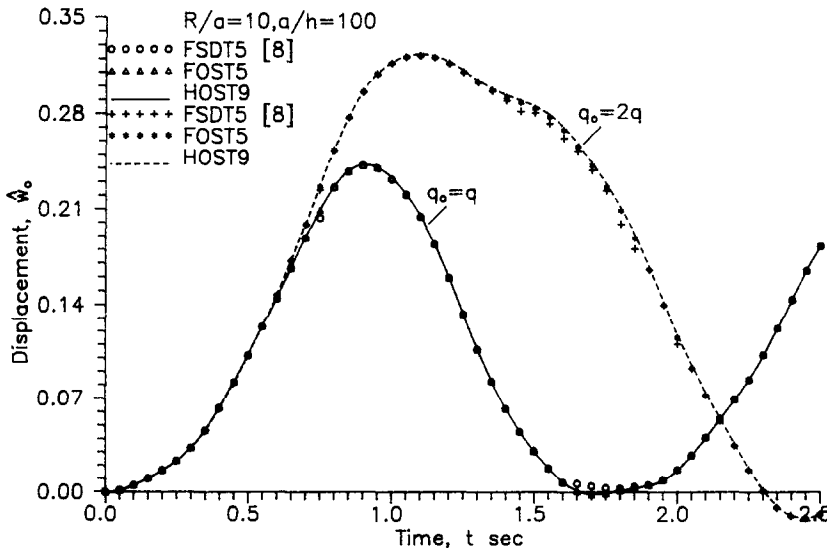


Fig. 5. Displacement vs time for a simply supported cross-ply ($0^\circ/90^\circ$) spherical shell subjected to a uniform transverse load ($q_0 = 1 \text{ N/cm}^2, \Delta t = 0.25 \times 10^{-3} \text{ sec}$).

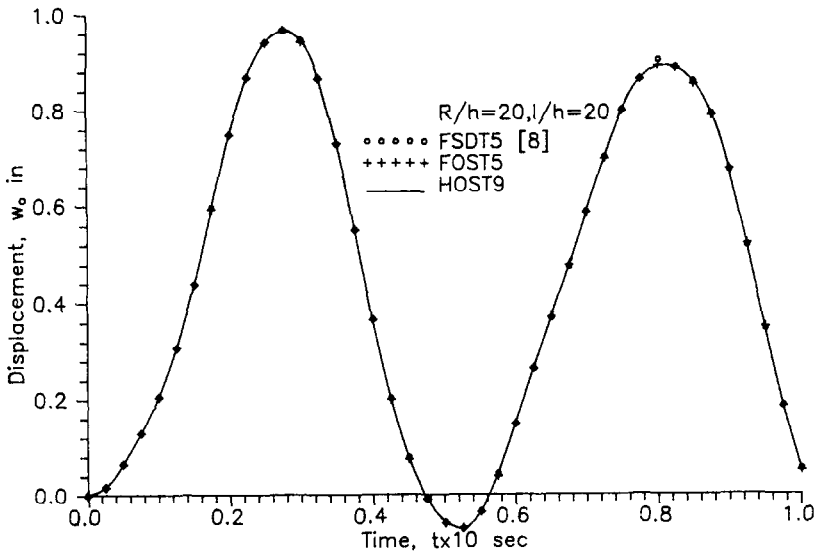


Fig. 6. Displacement vs time for a clamped cross-ply ($0^\circ/90^\circ$) cylindrical shell subjected to an internal pressure ($q_0 = 5000$ psi, $\Delta t = 100 \mu\text{sec}$).

varying pulse (i.e., in the time domain the variation is triangular as per eqn (24b) with a duration of $t_0 = 0.003$ sec) and a sinusoidally distributed load of maximum intensity 10,000 psi is considered. The variation of the central displacement with respect to time is presented in Fig. 7 for different lamination schemes. Even though the period of vibration does not change much, the peak amplitude decreases as θ increases to 45° and by further increasing θ the peak amplitude is increased. It is also observed that for $\theta = 30^\circ$ and $\theta = 60^\circ$ the results match each other exactly. The non-dimensional quantity used for representing the displacement here is

$$\hat{w}_0 = \left(\frac{w_0}{h} \right). \quad (27)$$

5. *A symmetric cross-ply spherical shell.* A simply supported cross-ply ($0^\circ/90^\circ/0^\circ$) spherical shell with material properties as per material set 1, $a/h = 10$ and for different R/a ratios 5, 10 and infinity, subjected to a triangular time varying pulse (i.e., in the time domain the variation is triangular as per eqn (24b) with a duration of $t_0 = 0.003$ sec), sinusoidal transverse load of maximum intensity 10,000 psi is considered. The effect of the shallowness of the shell on the central deflection of the spherical shell is investigated and the results are presented in Fig. 8. It is clear that a plate is relatively stiffer compared to a shell in the non-linear context. The non-dimensional quantity adopted for the displacement is as per eqn (27).

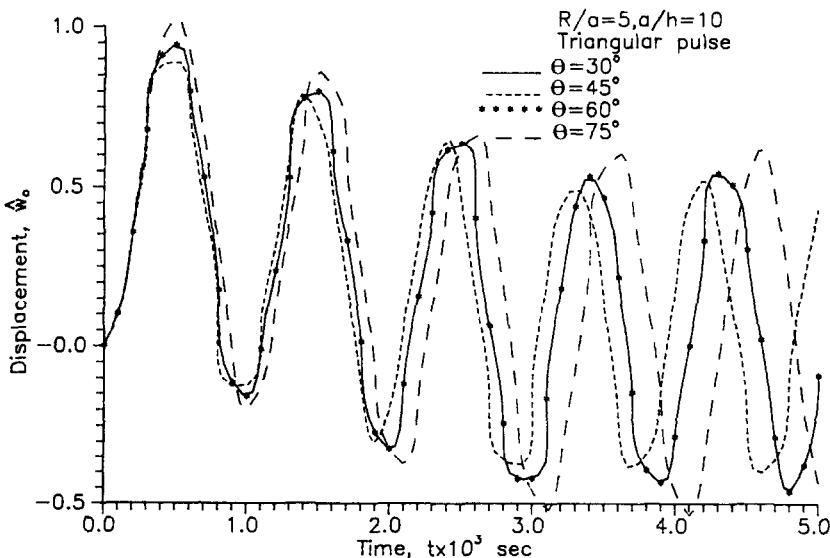


Fig. 7. Displacement vs time for a simply supported angle-ply ($\theta^\circ/\theta^\circ/\theta^\circ$) spherical shell subjected to a sinusoidal transverse load ($q_0 = 10,000$ psi, $t_0 = 0.003$ sec, $\Delta t = 2.5 \mu\text{sec}$).

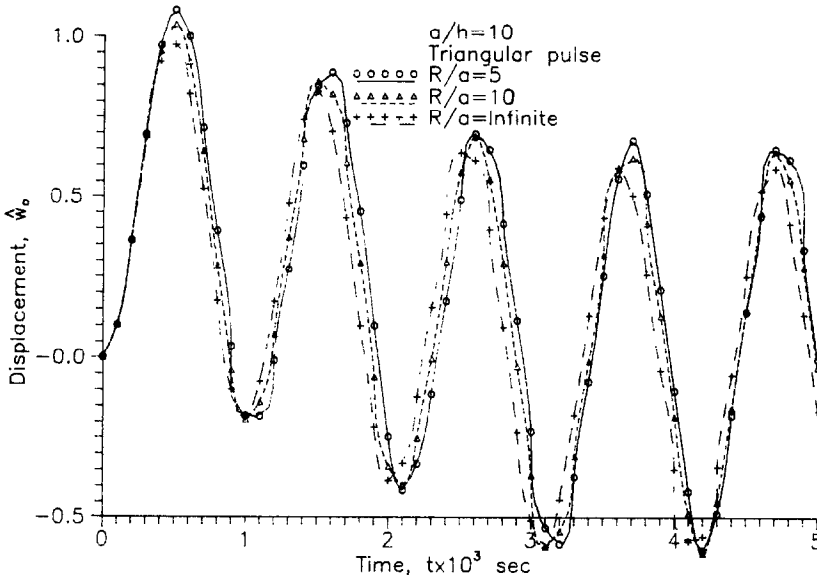


Fig. 8. Displacement vs time for a simply supported cross-ply (0°/90°/0°) spherical shell subjected to a sinusoidal transverse load ($q_0 = 10,000$ psi, $t_0 = 0.003$ sec, $\Delta t = 2.5 \mu\text{sec}$).

6. *A sandwich spherical shell with orthotropic factings.* A simply supported three layer sandwich spherical shell with geometry and material properties as per material set 4, subjected to a sinusoidal time varying (i.e., in the time domain the variation is sinusoidal as per eqn (24a) with a duration of $t_0 = 0.002$ sec), sinusoidal transverse load of maximum intensity $\hat{q}_0 = 64.1026$ is considered. The effect of shear deformation on the central displacement of the spherical shell is investigated and the results for different a/h ratios are presented in Fig. 9. It is observed that for $a/h = 100$ the predictions with both higher order shear deformation theory and first order shear deformation theory are exactly the same,

whereas for $a/h = 10$ the first order shear deformation theory underpredicts the displacements. This may be due to the predominant shear deformation effects in the case of thick sandwich shells. Hence this establishes the usefulness of the present higher order shear deformation theory in the predictions where shear deformation effects predominate. The non-dimensional quantities used are defined as follows:

$$\hat{q}_0 = \frac{q_0}{E_2} \left(\frac{a}{h}\right)^4; \quad \hat{w}_0 = \frac{w_0}{h};$$

$$\hat{\sigma}_x = \frac{\sigma_x}{E_2} \left(\frac{a}{h}\right)^2. \tag{28}$$

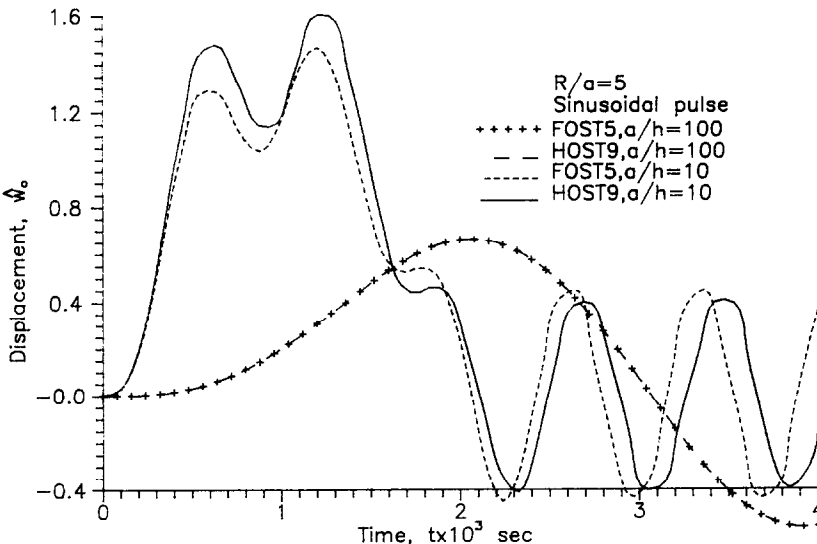


Fig. 9. Displacement vs time for a simply supported sandwich spherical shell subjected to a sinusoidal transverse load ($\hat{q}_0 = 64.1026$, $t_0 = 0.002$ sec, $\Delta t = 0.5 \mu\text{sec}$).

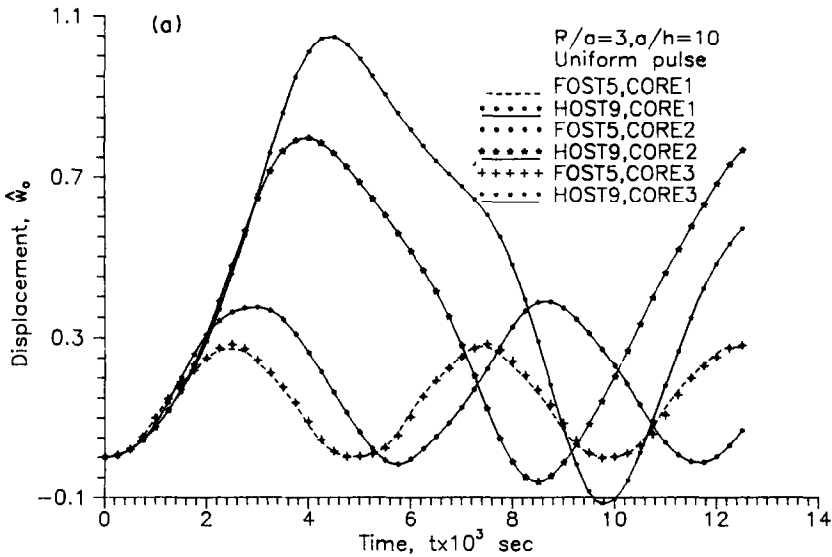


Fig. 10(a). Displacement vs time for a simply supported sandwich spherical shell with different core properties subjected to a uniform transverse load ($q_0 = 1000$ psi, $\Delta t = 25 \mu\text{sec}$).

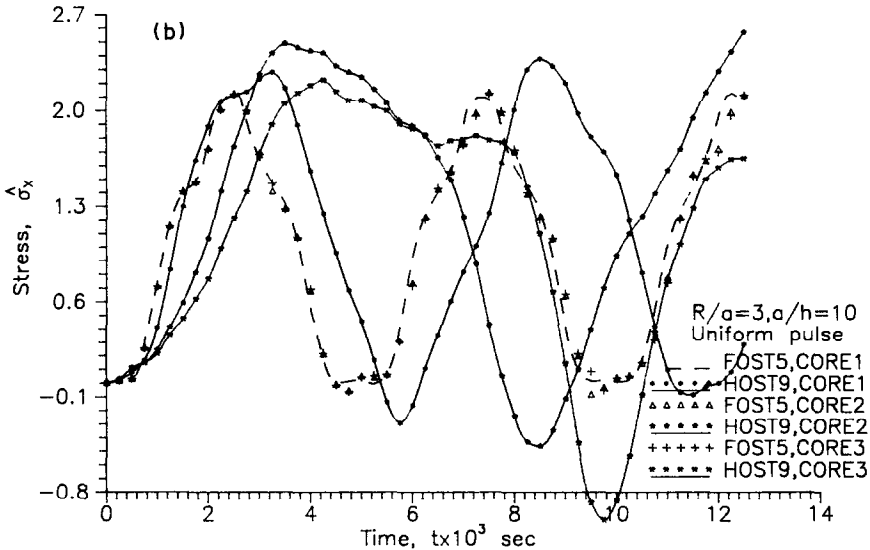


Fig. 10(b). Stress vs time for a simply supported sandwich spherical shell with different core properties subjected to a uniform transverse load ($q_0 = 1000$ psi, $\Delta t = 25 \mu\text{sec}$).

7. *A sandwich spherical shell with isotropic facings.* A simply supported sandwich spherical shell with geometry and material properties as per material set 5 subjected to an uniform pulse load of intensity $q_0 = 1000$ psi is considered. This problem is considered to investigate the effect of core properties on the central displacement and stresses and the results are presented in Figs 10(a) and 10(b). The non-dimensional quantities adopted are as per eqn (28). From the plots it is observed that when the core is progressively made weaker, the difference between first order shear deformation theory and higher order shear deformation theory predictions for displacement and stresses increases rapidly. It can be seen that not only the amplitude but also the period is affected. In

general, the effect is to soften the shell, thereby increasing the period of vibration. It is also observed that there is no variation in the predictions of first order shear deformation theory for different core properties. Thus the first order shear deformation theory is inadequate for sandwich shells for which the present higher order shear deformation theory can be used effectively.

CONCLUSIONS

The numerical results of the linear and geometrically non-linear transient analyses of isotropic, orthotropic and laminated composite and sandwich shells are presented. The simple C^0 isoparametric

formulation of an assumed higher order displacement model employed here is stable and accurate in predicting the linear and geometrically non-linear transient responses of laminated composite and sandwich shells. In contrast to first order shear deformation theory, the present theory does not require the usual shear correction factors generally associated with first order shear deformation theory. The present finite element results in the linear and geometrically non-linear analyses agree very well with the available closed-form two-dimensional solutions developed based on another higher order theory and other finite element solutions in the open literature.

It is observed that the effect of shear deformation in thick sandwich shells with a weak core and strong facings as well as laminated shells with large ratios of the tangential elastic modulus to the transverse shear modulus is considerable. It is believed that the refined shear deformation theory presented here is essential for predicting accurate responses especially for sandwich shells. The present results of the linear and geometrically non-linear analyses of sandwich laminates should serve as a reference for future investigations.

Acknowledgement—Partial support of this research by the Aeronautics Development Board, Ministry of Defence, Government of India through its Grant Nos. Aero/RD-134/100/10/88-89/518 and Aero/RD-134/100/10/88-89/534 is gratefully acknowledged.

REFERENCES

1. P. M. Naghdi, A survey of recent progress in the theory of elastic shells. *Appl. Mech. Rev.* **9**, 365–368 (1956).
2. G. Horrigmoe and P. G. Bergan, Incremental variational principles and finite element models for non-linear problems. *Comput. Meth. appl. Mech. Engng* **7**, 201–207 (1976).
3. S. C. Panda and R. Natarajan, Finite element analysis of laminated shells of revolution. *Comput. Struct.* **6**, 61–64 (1976).
4. K. N. Shivakumar and A. V. Krishna Murty, A higher precision ring element for vibrations of laminated shells. *J. Sound Vibr.* **58**, 311–318 (1978).
5. K. P. Rao, A rectangular laminated anisotropic shallow thin shell finite element. *Comput. Meth. appl. Mech. Engng* **15**, 15–33 (1978).
6. Y. S. Hsu, J. N. Reddy and C. W. Bert, Thermoelasticity of circular cylindrical shells laminated of bimodulus composite materials. *J. Thermal Sci.* **4**, 115–117 (1981).
7. J. N. Reddy, Bending of laminated anisotropic shells by a shear deformable finite element. *Fibre Sci. Technol.* **17**, 2–24 (1982).
8. J. N. Reddy and K. Chandrashekhara, Geometrically non-linear transient analysis of laminated, doubly curved shells. *Int. J. Non-linear Mech.* **20**, 79–90 (1985).
9. J. N. Reddy and K. Chandrashekhara, Non-linear finite element models of laminated plates and shells. In *Finite Elements in Computational Mechanics* (Edited by T. Kant), pp. 189–209. Pergamon Press, London (1985).
10. F. B. Hildebrand, E. Reissner and G. B. Thomas, Notes on the foundations of the theory of small displacements of orthotropic shells. NACA TN-1833 (1949).
11. T. Kant, Thick shells of revolution—some studies, Ph.D. thesis, Department of Civil Engineering, Indian Institute of Technology, Bombay, India (1976).
12. J. M. Whitney and C. T. Sun, A refined theory for laminated anisotropic cylindrical shells. *ASME J. appl. Mech.* **41**, 47–53 (1974).
13. T. Kant, A higher order general shell theory, Research Report, C/R/391/81, Civil Engineering Department, University of Wales, Swansea (1981).
14. T. Kant, A higher order general laminated shell theory. Research Report, C/R/395/81, Civil Engineering Department, University of Wales, Swansea (1981).
15. T. Kant, D. R. J. Owen and O. C. Zienkiewicz, A refined higher order C^0 plate bending element. *Comput. Struct.* **15**, 177–183 (1982).
16. J. N. Reddy, A simple higher order theory for laminated composite plates. *ASME J. appl. Mech.* **51**, 745–752 (1984).
17. J. N. Reddy and C. F. Liu, A higher order shear deformation theory of laminated elastic shells. *Int. J. Engng Sci.* **23**, 319–330 (1985).
18. J. N. Reddy and A. A. Khdeir, Dynamic response of cross-ply laminated shallow shells according to a refined shear deformation theory. *J. Acoust. Soc. Amer.* **85**, 2423–2431 (1989).
19. T. Kant and J. R. Kommineni, Geometrically non-linear analysis of doubly curved laminated and sandwich fibre reinforced composite shells with a higher order theory and C^0 finite elements. *J. Reinfr. Plast. Comp.* **11**, 1048–1076 (1992).
20. T. Kant and Mallikharjuna, Non-linear dynamics of laminated plates with a higher order theory and C^0 finite elements. *Int. J. Non-linear Mech.* **26**, 335–343 (1991).
21. T. Kant and M. P. Menon, Higher order theories for composite and sandwich cylindrical shells with C^0 finite elements. *Comput. Struct.* **33**, 1191–1204 (1989).
22. T. Kant and M. P. Menon, Estimation of interlaminar stresses in fibre reinforced composite cylindrical shells. *Comput. Struct.* **38**, 131–147 (1991).
23. Mallikharjuna and T. Kant, Finite element transient analysis of composite and sandwich plates based on a refined higher order theory. *ASME J. appl. Mech.* **57**, 1084–1086 (1990).
24. T. Kant, R. V. Ravichandran, B. N. Pandya and Mallikharjuna, Finite element transient analysis of isotropic and fibre reinforced composite plates using a higher order theory. *Compos. Struct.* **9**, 319–342 (1988).
25. T. Kant and Mallikharjuna, Transient dynamics of composite sandwich plates using 4, 8, 9 noded isoparametric quadrilateral elements. *Finite Elem. Anal. Design* **6**, 307–318 (1989).
26. T. Kant and S. Patel, Transient/pseudo-transient finite element small/large deformation analysis of two dimensional problems. *Comput. Struct.* **36**, 421–427 (1990).
27. T. Kant, J. H. Varaiya and C. P. Arora, Finite element transient analysis of composite and sandwich plates based on a refined theory and implicit time integration schemes. *Comput. Struct.* **36**, 401–420 (1990).
28. T. Kant, On finite element discretization of a higher order shell theory. In *The Mathematics of Finite Elements and Applications IV* (MAFELAP 1981) (Edited by J. R. Whiteman), pp. 209–217. Academic Press, London (1982).
29. T. Kant, Transient dynamics of fibre reinforced composite plates. Research Report, IIT-B/CE/RR/87/1, Indian Institute of Technology, Bombay, India (1987).
30. T. Kant and B. N. Pandya, A simple finite element formulation of a higher order theory for unsymmetrically laminated composite plates. *Compos. Struct.* **9**, 215–246 (1988).
31. V. V. Novozhilov, *Foundations of the Non-linear Theory of Elasticity*. Graylock Press, Rochester, New York (1953).
32. O. C. Zienkiewicz, *The Finite Element Method*, 3rd Edn. McGraw-Hill, London (1977).

33. E. Hinton, T. A. Rock and O. C. Zienkiewicz, A note on mass lumping and related process in the finite element method. *Earthqu. Engng Struct. Dyn.* **4**, 245–249 (1976).
34. T. Y. Tsui and P. Tong, Stability of transient solutions of moderately thick plates by finite difference methods. *AIAA J.* **9**, 2062–2063 (1971).
35. V. P. Iu, Y. K. Cheung and S. C. Lau, Non-linear vibration analysis of multi-layered beams by finite element analysis. *J. Sound Vibr.* **100**, 359–362 (1985).
36. K. J. Bathe, E. Ramm and E. L. Wilson, Finite element formulation for large deformation dynamic analysis. *Int. J. Numer. Meth. Engng* **19**, 353–362 (1975).
37. T. Kant, B. S. Manjunatha, M. P. Menon and J. R. Kommineni, Refined higher order laminate theories: a historical perspective. *Proc. 36th Congress of the Indian Society of Theoretical and Applied Mechanics*, Indian Institute of Technology, Bombay (1991).